Interaction of two-color solitary waves in a liquid crystal in the nonlocal regime

Benjamin D. Skuse* and Noel F. Smyth†

School of Mathematics and Maxwell Institute for Mathematical Sciences, University of Edinburgh, The King's Buildings, Edinburgh, Scotland EH9 3JZ, United Kingdom

(Received 3 November 2008; revised manuscript received 5 January 2009; published 3 June 2009)

The propagation and interaction of two-color vector solitary waves in a nematic liquid crystal in the nonlocal nonlinear response regime are investigated. Approximate modulation equations governing the evolution of the beams are derived based on a variational method. These modulation equations are then extended to include the effect of the diffractive radiation shed by the beams as they evolve. Agreement between the approximate solutions and full numerical solutions of the governing equations for the momentum deviation due to diffraction is excellent. Moreover, radiative losses are shown to play a far less significant role with respect to momentum deviation in comparison with the case for the local regime.

DOI: 10.1103/PhysRevA.79.063806 PACS number(s): 42.65.Tg, 42.70.Df

I. INTRODUCTION

Spatial optical solitons (SOSs) have been studied intensively in the past few years due to their potential application in all-optical communication systems [1–3]. The waveguiding ability of SOS, combined with the retention of their basic size and shape, suggests the potential for their use in reconfigurable photonic circuits which could theoretically be constructed without the need for permanent guiding structures [4,5]. In a series of experimental and theoretical works Assanto and co-workers [6–10] demonstrated the existence of (2+1)-dimensional SOS in nematic liquid crystals (NLCs), which they termed nematicons, for which the nonlocal, anisotropic, nonlinear response of the medium balances the diffraction of the beam. The stability of these nematicons was proven theoretically by Conti *et al.* [6], where it was found to be due to the nonlocal nature of the nematicon's interaction with the medium. Nonlocality in this sense refers to the reorientational response of the medium to the nematicon(s) having a width much greater than the width of the light beam(s). Nonlinear nonlocal equations similar to those governing nematicons have been found to govern solitary waves in other media, for instance, colloidal suspensions [11,12], media with optical thermal nonlinearity [13,14], and photorefractive media [15,16]. In the highly nonlocal limit, effectively infinite nonlocality, Snyder and Mitchell [17] showed that SOSs are governed by a linear Schrödinger equation and that a SOS has a Gaussian profile. This linear equation in the highly nonlocal limit allowed stability of a SOS to be shown [18]. Additionally, the equations governing nematicons are the same as those governing a thermoelastic waveguide, for which Kuznetsov and Rubenchik [14] showed that solitary waves are stable.

Many proposed all-optical devices would include two or more SOSs interacting [1,2,19]. Since nematic liquid crystals form an ideal test bed for such devices, an important area of current research is multinematicon interaction behavior [2,19,20]. In particular, the nonlocal nature of the NLC response means that the nematicons exhibit interactions even when separated beyond any overlap of their transverse profiles [1,19]. Interesting phenomena have been observed experimentally including beam fusion, pulse-splitting, annihilation, and spinning [3,5,19–22].

In the present work the formation and propagation of a bound two-color vector nematicon formed from the interaction of two nematicons of different wavelengths (colors) will be investigated. These two nematicon beams of different wavelengths experience different degrees of diffraction and nematic coupling which, in the linear limit, leads to beam splitting. However, the interaction through the (nonlocal) nematic results in a mutual attraction and a self-localized vector solitary wave, or two-color nematicon, can then form under suitable boundary conditions. Recently, Alberucci *et al.* [2] experimentally observed these two-color nematicons. In this work they derived the governing equations for the propagation of the two beams and compared numerical solutions of these equations with experimental results [2].

The dynamics of two-color nematicon interactions in the nonlocal limit will be studied using a variational method based on that of Minzoni *et al.* [23] for a single nematicon. Modulation equations for the evolution of the beams are derived by inserting a suitable trial function into an averaged Lagrangian formulation of the governing equations. These modulation equations are then extended to include the effect of the diffractive radiation shed by the beams as they evolve [20,23–27]. Skuse and Smyth [27] found that for two-color nematicon interactions in the local regime the inclusion of this radiation is essential in order to obtain good agreement between numerical and modulation solutions. In particular, they found that the momentum deviation critically depends on the inclusion of these radiative losses [27]. Without the inclusion of this radiation, the modulation momentum deviation differed from the numerical one by up to 30%, while when the radiation was included the difference was no more than 1%. Here the term momentum deviation refers to a diffraction effect rather than optical anisotropy, the angular deviation of the Poynting vector from the wave vector. It is then the off-axis departure of each color (beam) component as it undergoes a different amount of diffraction while the system conserves linear (and angular) momentum. In particular the momentum deviation is independent of the Poyn-

*b.d.skuse@sms.ed.ac.uk
†n.smyth@ed.ac.uk

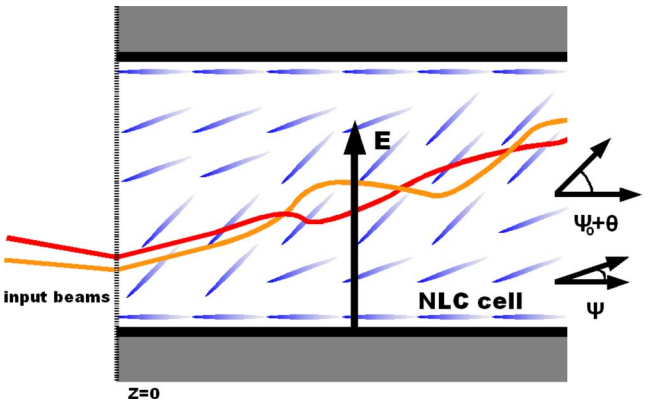

FIG. 1. (Color online) Schematic diagram of a liquid crystal cell with two polarized light beams of different colors.

ting vector walk-off and has no relation to it. In the present nonlocal limit the effect of the diffractive radiation shed by the beams as they evolve is shown to be far less significant in obtaining good agreement between numerical and approximate solutions, particularly with regard to momentum deviation, in agreement with experimental reports [22]. Excellent agreement is found between the numerical and modulation solutions, with the momentum deviation agreeing to within 2%. The present work then forms the nonlocal complement to the work of Skuse and Smyth [27] for the local limit. In this regard two points should be noted. One is that the material response in the nonlocal limit is fundamentally different to that in the local limit. In the local limit (2+1)-dimensional solitary waves are stable due to the governing equations reducing to a saturating nonlinear Schrödinger (NLS) equation, while in the nonlocal limit stability is due to the nonlocal material response. The second point is that the present work is concerned with experimental values of the nonlocality, for which the highly nonlocal asymptotic limit of Snyder and Michell [17] is not always valid [28].

II. APPROXIMATE EQUATIONS

Alberucci *et al.* [2] considered two polarized coherent light beams of different colors (wavelengths) propagating through a nematic liquid crystal cell in the absence of an external static electric field. In an extension of this experimental setup, an externally applied static electric field E, as sketched in Fig. 1, can be introduced to overcome the Freédericksz threshold [6,29]. The cell geometry is illustrated in Fig. 1. The direction down the cell is z with the (x,y) plane orthogonal to this. The input light beams are polarized so that their electric fields are in the x direction. The Freédericksz threshold is overcome by applying a static electric field in the x direction which causes the optical director angle to be pretilted by an angle ψ_0 to the z direction. Typically ψ_0 is around $\pi/4$, for example, 30° [30], as $\psi_0=\pi/4$ reduces the Freédericksz threshold to zero [6]. When light beams are incident, the optical director angle is perturbed by a further angle θ. In the present work we shall be interested in the small optically induced rotation limit, so that the total director angle is $\psi=\psi_0+\theta$, where $|\theta| \ll |\psi_0|$. On setting the nematicon equations [2] in nondimensional form, the nondimensional equations governing two-color nematicon propagation in the presence of an applied static pretilting electric field are

$$i\frac{\partial u}{\partial z}+\frac{1}{2}D_u\nabla^2 u+A_u u \sin 2\theta=0, \tag{1}$$

$$i\frac{\partial v}{\partial z}+\frac{1}{2}D_v\nabla^2 v+A_v v \sin 2\theta=0, \tag{2}$$

$$q \sin 2\theta-2\cos 2\theta(A_u|u|^2+A_v|v|^2)=\nu\nabla^2\theta, \tag{3}$$

where the Laplacian ∇^2 is in the (x,y) plane [6,31,32]. The variables u and v are the complex-valued slowly varying envelopes of the electric fields of the two beams, modified by a phase factor discussed below. The Poynting vector walk-off is accounted for in the electric field equations [Eqs. (1) and (2)] via a phase transformation. If Δ_u and Δ_v are the walk-off angles for each color, then the actual electric field envelopes are obtained from u and v by multiplying u by the phase factor $\exp\{[(i/2)z\tan^2\Delta_u-ix\tan\Delta_u]/D_u\}$ and a symmetric expression for v [33]. These phase factors give the beam trajectories a tilt from the z direction corresponding to the Poynting vector walk-off, accounting for the deviation of the Poynting vector from the wave vector. A_k and D_k are coupling and diffraction coefficients, respectively, where $k=u,v$. Finally q is given in terms of the square of the pretilting field by

$$q=\frac{4\Delta\epsilon_{RF}}{\epsilon_0 n_a^2 A^2\tan 2\psi_0}E^2, \tag{4}$$

with $\Delta\epsilon_{RF}$ as the low-frequency anisotropy, $n_a^2=n_\parallel^2-n_\perp^2$ as the optical anisotropy, and A as a scale amplitude of the input beam [6,34], and ν measures the strength of the response of the nematic and so measures its degree of nonlocality, with a nonlocal response corresponding to ν large.

Equations (1) and (2) are clearly coupled nonlinear Schrödinger-type (CNLS-type) equations for each color beam and Eq. (3) is a director (Poisson) equation which governs the reorientation of the electric fields [2].

In the nonlocal ν large limit, it can be seen from the director equation [Eq. (3)] that θ, the optically induced deviation of the optical director angle from ψ_0, is small for input beam powers that are not large. Let us then assume optical powers and nonlocality ν for which $|\theta|$ is small, so that the governing equations may be approximated by

$$i\frac{\partial u}{\partial z}+\frac{1}{2}D_u\nabla^2 u+2A_u u\theta=0, \tag{5}$$

$$i\frac{\partial v}{\partial z}+\frac{1}{2}D_v\nabla^2 v+2A_v v\theta=0, \tag{6}$$

$$2q\theta-2(A_u|u|^2+A_v|v|^2)=\nu\nabla^2\theta. \tag{7}$$

Since no exact solutions of Eqs. (5)–(7) exist, alternative methods must be used to study the evolution of the two-color nematicons. One such successful method is that based on

modulation equations derived from an averaged Lagrangian [20,21,23–27]. This method will be used in the present work and the solutions of the modulation equations will be compared with full numerical solutions of the governing equations. The two-color nematicon [Eqs. (5)–(7)] have the Lagrangian

$$L = \sum_{k=u,v} [i(k^* k_z - k k_z^*) - D_k |\nabla k|^2 + 4A_k \theta |k|^2] - \nu |\nabla \theta|^2 - 2q\theta^2. \tag{8}$$

Appropriate trial functions are then inserted into the averaged Lagrangian

$$\mathcal{L} = \int_{-\infty}^{\infty} \int_{-\infty}^{\infty} L dx dy, \tag{9}$$

from which variational equations are derived for the beam parameters. Gaussians have been widely employed as trial functions for SOS in the highly nonlocal limit [35,36]. However in Sec. III it will be shown that for experimental values of ν, a Gaussian profile does not give good agreement with numerical solutions, while a sech profile does. Suitable trial functions for nonspinning nematicons are then

$$k = a_k \operatorname{sech} \frac{\chi_k}{w_k} e^{i\psi_k} + i g_k e^{i\psi_k}, \quad k = u,v,$$

$$\theta = \sum_{k=u,v} \alpha_k \operatorname{sech}^2 \frac{\chi_k}{\beta_k}, \tag{10}$$

where

$$\chi_k = \sqrt{(x-\xi_k)^2 + y^2}, \quad \psi_k = \sigma_k + V_k (x - \xi_k) \tag{11}$$

and the nematicon parameters are functions of z, these being the electric field amplitudes a_k and widths w_k, nematicon positions ξ_k, velocities V_k, phases σ_k, shelf amplitudes g_k, and director beam amplitudes α_k and widths β_k, where $k = u,v$. The first terms in the trial functions for u and v represent varying solitonlike beams, while the second terms represent the diffractive radiation of low wave number which accumulates under the evolving nematicons [23,24]. This radiation cannot remain flat, so it is assumed that g_k are nonzero in the disks, $0 \le \sqrt{(x-\xi_k)^2 + y^2} \le R_k$ [23,24]. The form of the diffractive radiation outside of these disks will be discussed at the end of this section.

Modulation equations for the nematicon parameters are now found by substituting trial function (10) into the averaged Lagrangian (9), the modulation equations being obtained as variational equations with respect to the nematicon parameters. The resulting calculations are as in Assanto *et al.* [21], so the details will not be reported here. These modulation equations can then be augmented to include the effect of the diffractive radiation shed as the nematicons evolve [21,23,26]. The final modulation equations for the nematicon parameters are, in this manner,

$$\frac{d}{dz}(I_2 a_u^2 w_u^2 + \Lambda_u g_u^2) = -2 D_u \delta_u \tilde{\Lambda}_u \kappa_u^2, \tag{12}$$

$$I_1 \frac{d}{dz}(a_u w_u^2) = \Lambda_u g_u \left(\sigma_u - \frac{1}{2} D_u V_u^2 \right), \tag{13}$$

$$\frac{d\xi_u}{dz} = D_u V_u, \tag{14}$$

$$I_1 \frac{dg_u}{dz} = \frac{1}{2} D_u I_{22} a_u w_u^{-2} - A_u A^2 B^4 a_u w_u^2 [\alpha_u \beta_u^2 Q_1^{-2} + \alpha_v \beta_v^2 Q_2^{-2} e^{-\gamma_1} - \alpha_v \beta_v^2 \rho^2 Q_2^{-3} e^{-\gamma_1}] - 2 D_u \delta_u g_u, \tag{15}$$

$$I_2 a_u^2 w_u^2 \left(\frac{d\sigma_u}{dz} - \frac{1}{2} D_u V_u^2 \right) = -I_{22} D_u a_u^2 + A_u A^2 B^2 a_u^2 w_u^2 \{\alpha_u \beta_u^2 (A^2 \beta_u^2 + 2B^2 w_u^2) Q_1^{-2} + \alpha_v \beta_v^2 [(A^2 \beta_v^2 + 2B^2 w_u^2) Q_2 - w_u^2 \rho^2] Q_2^{-3} e^{-\gamma_1}\}, \tag{16}$$

$$\frac{d}{dz}[(I_2 a_u^2 w_u^2 + \Lambda_u g_u^2) V_u] = -2 A_u A^2 B^2 \alpha_v a_u^2 w_u^2 \beta_v^2 \rho Q_2^{-2} e^{-\gamma_1} - 2 A_v A^2 B^2 \alpha_u a_v^2 w_v^2 \beta_u^2 \rho Q_4^{-2} e^{-\gamma_2} + 2 \alpha_u \alpha_v \beta_u^2 \beta_v \rho \times [2(2 - \rho^2 Q_5^{-1}) A^{-2} Q_5^{-1} + q] Q_5^{-2} e^{-\gamma_3}, \tag{17}$$

the algebraic equations

$$2(\nu I_{42} + q I_4 \beta_u^2) \alpha_u = A_u A^2 B^2 a_u^2 w_u^2 \beta_u^2 Q_1^{-1} + A_v A^2 B^2 a_v^2 w_v^2 \beta_u^2 Q_4^{-1} e^{-\gamma_2} - \frac{\alpha_v \beta_u^2 \beta_v^2}{Q_5} \left[\frac{2\nu}{Q_5} \left(1 - \frac{\rho^2}{A^2 Q_5} \right) - q A^2 \right] e^{-\gamma_3}, \tag{18}$$

$$q I_4 \alpha_u = A_u A^2 B^4 a_u^2 w_u^4 Q_1^{-2} + A_v A^2 B^2 a_v^2 w_v^2 (B^2 w_v^2 + A^2 \beta_u^2 \rho^2) Q_4^{-2} e^{-\gamma_2} + \frac{2\nu \alpha_v \beta_v^2}{Q_5^3} \left[\beta_v^2 - \beta_u^2 - \frac{\rho^2}{A^2 Q_5} \times \left(\beta_v^2 - 3\beta_u^2 - \frac{\beta_u^2 \rho^2}{A^2 Q_5} \right) \right] e^{-\gamma_3} - q \alpha_v \beta_u \beta_v^2 (A^2 \beta_v^2 + \beta_u \rho^2 Q_5^{-1}) Q_5^{-2} e^{-\gamma_3}, \tag{19}$$

plus the symmetric modulation equations for the v color.

In these equations,

$$\Lambda_u = R_u^2/2, \quad A = \frac{I_2 \sqrt{2}}{\sqrt{I_{x32}}}, \quad B = \sqrt{2 I_2},$$

$$Q_1 = A^2 \beta_u^2 + B^2 w_u^2, \quad Q_2 = A^2 \beta_v^2 + B^2 w_u^2,$$

$$Q_3 = A^2 \beta_v^2 + B^2 w_v^2, \quad Q_4 = A^2 \beta_u^2 + B^2 w_v^2,$$

$$Q_5 = \beta_u^2 + \beta_v^2, \quad \gamma_1 = \frac{\rho^2}{Q_2}, \quad \gamma_2 = \frac{\rho^2}{Q_4},$$

$$\gamma_3 = \frac{\rho^2}{A^2 Q_5} \quad \text{and} \quad \rho = \xi_u - \xi_v. \tag{20}$$

The integrals I_i and I_{ij} are

$$I_1 = \int_0^\infty x \operatorname{sech} x dx = 2C,$$

$$I_2 = \int_0^\infty x \operatorname{sech}^2 x dx = \ln 2,$$

$$I_{22} = \int_0^\infty x \operatorname{sech}^2 x \tanh^2 x dx = \frac{1}{3}\ln 2 + \frac{1}{6},$$

$$I_{x32} = \int_0^\infty x^3 \operatorname{sech}^2 x dx = 1.352\ 301\ 002\cdots,$$

$$I_{42} = \frac{1}{4}\int_0^\infty x\left[\frac{d}{dx}\operatorname{sech}^2 x\right]^2 dx = \frac{2}{15}\ln 2 + \frac{1}{60}, \tag{21}$$

where C is the Catalan constant, $C=0.915\ 965\ 594\cdots$ [37]. Modulation Eqs. (12) and (15) contain terms representing loss to shed diffractive radiation. In these equations the loss coefficient δ_u is

$$\delta_u = -\frac{\sqrt{2\pi} I_1}{2e\kappa_u \tilde{\Lambda}_u}\int_0^z \pi\kappa_u(z')\ln[(z-z')/\tilde{\Lambda}_u] \times \left[\left(\left\{\frac{1}{2}\ln[(z-z')/\tilde{\Lambda}_u]\right\}^2 + \frac{3\pi^2}{4}\right)^2 + \pi^2\{\ln[(z-z')/\tilde{\Lambda}_u]\}^2\right]^{-1}\frac{dz'}{(z-z')}. \tag{22}$$

Finally,

$$\kappa_u^2 = \frac{1}{\tilde{\Lambda}_u}[I_2 a_u^2 w_u^2 - I_2 \hat{a}_u^2 \hat{w}_u^2 + \tilde{\Lambda}_u g_u^2], \tag{23}$$

where

$$\tilde{\Lambda}_u = \tfrac{1}{2}(7\beta_{u1/2})^2, \quad \beta_{u1/2} = \beta_u \operatorname{sech}^{-1}(1/\sqrt{2}). \tag{24}$$

In expression (23) for κ_u the caret denotes fixed point values, which will be discussed below.

Modulation Eqs. (12)–(19) form a conservative system when loss to diffractive radiation is neglected, so that $\delta_u = \delta_v = 0$. A number of details of the evolution of the nematicons can be found from conservation equations resulting from this neglect of shed radiation. On ignoring diffractive loss, Eqs. (12) and (17) are mass conservation and momentum equations for the color u in the sense of invariances of Lagrangian (8) [38]. Adding momentum Eq. (17) in the u color to its symmetric counterpart in the v color gives the equation for total momentum conservation as

$$\frac{d}{dz}\sum_{k=u,v}(I_2 a_k^2 w_k^2 + \Lambda_k g_k^2)V_k = 0. \tag{25}$$

In addition to this momentum conservation equation, the modulation equations also possess an energy conservation equation. This energy conservation equation is found from Nöther's theorem as a consequence of the z invariance of Lagrangian (8) [21] and is

$$\frac{dH}{dz} = \frac{d}{dz}\Bigg\{-2A_u A^2 B^2 \alpha_v a_u^2 w_u^2 \beta_v^2 Q_2^{-1} e^{-\gamma_1} - 2A_v A^2 B^2 \alpha_u a_v^2 w_v^2 \beta_u^2 e^{-\gamma_2} Q_4^{-1} + 4\nu\alpha_u\alpha_v\beta_u^2\beta_v^2 \times (1-\rho^2 Q_5^{-1}) Q_5^{-2} e^{-\gamma_3} + 2qA^2\alpha_u\alpha_v\beta_u^2\beta_v^2 Q_5^{-1} e^{-\gamma_3} + \sum_{k=u,v}\Bigg[I_{22} D_k a_k^2 + D_k(I_2 a_k^2 w_k^2 + \Lambda_k g_k^2)V_k^2 - \frac{2A_k A^2 B^2 \alpha_k a_k^2 w_k^2 \beta_k^2}{(A^2\beta_k^2 + B^2 w_k^2)} + 4\nu I_{42}\alpha_k^2 + 2qI_4\alpha_k^2\beta_k^2\Bigg]\Bigg\} = 0. \tag{26}$$

The fixed points of modulation Eqs. (12)–(19) are the steady nematicon solutions of the governing equations. There are two types of fixed points. The first type occurs when the nematicons interact and then pass through one another, resulting in separate single nematicons. The second type forms as a coupled vector nematicon as $z\to\infty$ with $\xi=\xi_u=\xi_v$. In the present work the latter type is the case of interest. With fixed point values of the pulse parameters denoted with a caret and boundary values at $z=0$ by a subscript 0, we then have $\hat{\xi}_u = \hat{\xi}_v$, $\hat{g}_u = \hat{g}_v = 0$, and $g_{u0} = g_{v0} = 0$. When diffractive radiation loss is ignored, so that $\delta_u = 0$ and $\delta_v = 0$, the modulation equations give an expression for the momentum deviation of the steady coupled vector nematicon. Using the momentum conservation Eq. (25), the mass conservation Eq. (12) with $\delta_u = 0$, and the position Eq. (14) and their v counterparts, the combined momentum deviation of the vector nematicon is

$$\hat{\xi}' = \hat{\xi}_u' = \hat{\xi}_v' = \frac{D_u D_v M_0}{I_2(D_u a_{v0}^2 w_{v0}^2 + D_v a_{u0}^2 w_{u0}^2)}, \tag{27}$$

where

$$M_0 = I_2 \sum_{k=u,v} a_{k0}^2 w_{k0}^2 V_{k0} \tag{28}$$

is the initial total momentum, which is conserved. In experiments the diffraction coefficients D_k and the coupling coefficients A_k take similar values. For instance, for the experiments of Alberucci *et al.* [2] the diffraction coefficients were 0.805 for red and 0.823 for near-infrared light. An approximation to the fixed points of the modulation equations can then be found by taking $D_u = D_v$ and $A_u = A_v$ and using the energy conservation Eq. (26) [21,27]. This fixed point is required in the calculation of the shed radiation [see expression (23)], arising from the diffractive radiation loss.

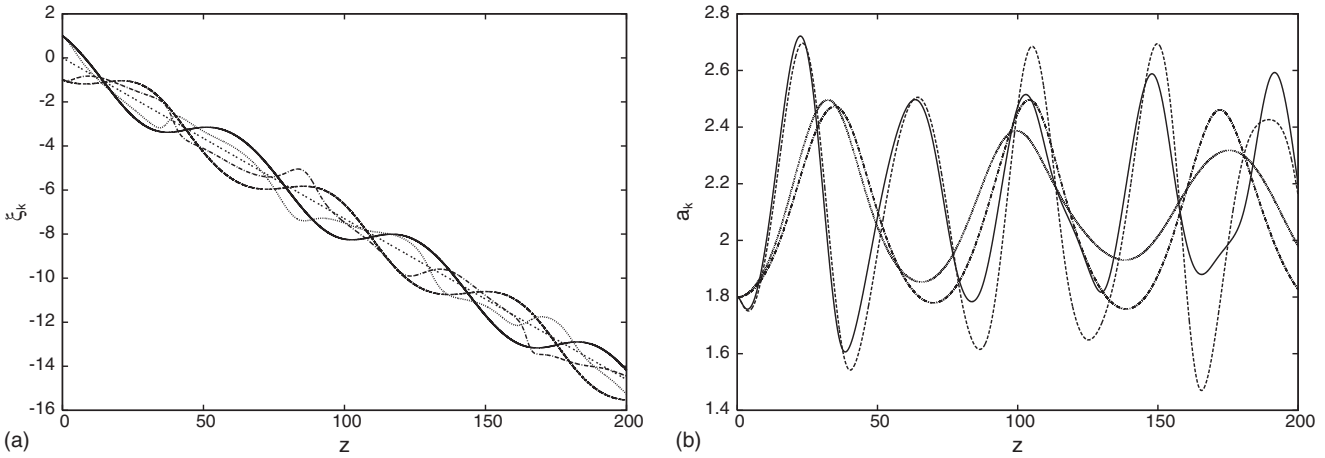

FIG. 2. Comparisons for the initial values $a_u=a_v=1.8$, $w_u=w_v=3.0$, $\xi_u=1.0$, $\xi_v=-1.0$, $V_u=0.1$, and $V_v=-0.05$ with $\nu=500$, $q=2$, $A_u=1.0$, $A_v=0.95$, $D_u=1.0$, and $D_v=0.98$. Full numerical solution u color (—), v color (– – –); solution of modulation equations for u color (···), v color (–·–·–); (a) Positions and momentum conservation result (27) (·· ··); (b) amplitudes.

III. RESULTS AND COMPARISONS WITH NUMERICAL SOLUTIONS

In this section full numerical solutions of two-color nematicon Eqs. (1)–(3) will be compared with solutions of the modulation equations. Field Eqs. (1) and (2) were solved using a pseudospectral method similar to that of Fornberg and Whitham [39]. Director Eq. (3) was solved as a boundary value problem using a Fourier method [40]. The numerical method is the same as that of Skuse and Smyth [27], so no further description will be given here. The modulation equations were solved using the standard fourth-order Runge-Kutta scheme. The initial condition used for the full numerical solutions was trial function (10) for u and v, with $g_k=0$ and $\sigma_k=0$. The initial director distribution is then determined by solving Poisson Eq. (3) with these initial u and v. The mean momentum deviation was found from the numerical solution by solving to a large value of z, then plotting the intersection points of the colors. Linear regression was then applied to determine the mean propagation direction, from which the mean momentum deviation was obtained.

Equations (5)–(7) are approximations to nematicon Eqs. (1)–(3) where it has been assumed that θ is small enough that the first terms of the Taylor series of $\sin 2\theta$ and $\cos 2\theta$ may be taken. This assumption is, however, only valid for highly nonlocal media for which $\nu>100$ for nondimensional optical powers of O(1) since the angle θ decreases as the degree of nonlocality ν increases. As a result, $\nu=500$ has been taken, which is a value at the upper end of the experimental range [4,6]. In addition it was found that Gaussian trial functions require much higher values of ν than sech trial functions for θ to be sufficiently small so that linearized Eqs. (5)–(7) are valid. It was found that Gaussian trial functions required $\nu>2000$, which is well outside the experimental range. Hence no results for Gaussian trial functions will be reported here. Above $\nu=2000$ the solutions were very similar to those for trial function (10). This is in accord with the Snyder-Mitchell asymptotic solution [17] which shows that a Gaussian becomes a better approximation to the nematicon profile as ν increases.

Figure 2 shows a comparison between the full numerical and modulation solutions for boundary values for which the beams evolved into a bound vector nematicon. It can be seen from Fig. 2(a) that the position comparison is excellent. The momentum deviation as given by the modulation and numerical solutions is in near perfect agreement. Also, unlike in the local case [27], the maxima and minima and the period of the position oscillations are in very good agreement. In the local regime, as the beams approach a collision they experience a sudden acceleration accompanied by radiative losses, which result in a rapid reduction in peak position oscillations [27]. However, nonlocal nematicon collisions do not involve such rapid accelerations because the beams interact at both distance due to the nematic and upon collision. The amplitude comparison shown in Fig. 2(b) is not as good. The modulation and numerical solutions agree in the mean, but the damping of the oscillations of the modulation solution is larger than that of the numerical solution. As the modulation equations form a nonlinear oscillator, this means that the modulation period is also larger than the numerical period. It is then apparent that the radiation calculation of Sec. II overestimates the effect of the shed radiation.

Figure 3 shows the numerical u color solution at $z=100$ and $y=0$ for $\nu=250$, $\nu=500$, and $\nu=1000$. As ν increases the deviation of the director angle θ decreases. Królikowski and Bang [41] found that in similar media an increase in nonlocality ν for fixed amplitude causes the width of the resultant beam to increase. Here broadening of the beam is clearly seen, as is a marked decrease in the final amplitude. The effect of acceleration is shown by the asymmetry of the radiation shelves near the tails of the beams. It can be seen that symmetry increases as nonlocality grows. There is also a noticeable reduction in the peak of the radiation shelves as ν increases. This figure confirms the conclusion that acceleration of the beams and radiative losses from the beams decrease as ν increases, the latter in agreement with experimental observations [22]. While the modulation solutions' positions reveal a harmonic oscillation, the numerical position exhibits more complicated behavior. As the degree of nonlocality is increased, from $\nu\sim100$ to $\nu\sim1000$, harmonicity of the numerical position oscillation increases. Nem-

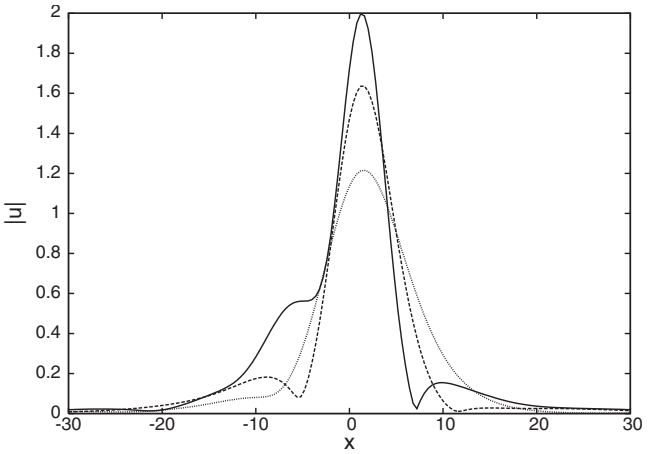

FIG. 3. Full numerical beam profile comparison at $z=100$ and $y=0$ for the initial values $a_u=a_v=1.2$, $w_u=w_v=4.0$, $\xi_u=1.0$, $\xi_v=-1.0$, and $V_u=0.1$ with $q=2$, $A_u=1.0$, $A_v=0.95$, $D_u=1.0$, and $D_v=0.98$. Solution for $\nu=250$ (—), solution for $\nu=500$ (– – –), and solution for $\nu=1000$ (···).

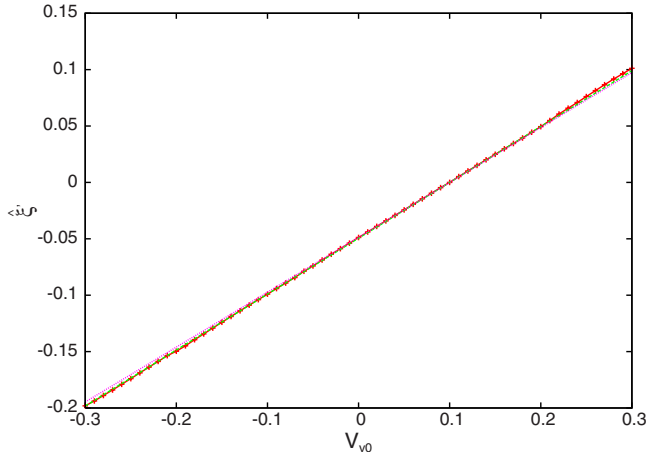

FIG. 4. (Color online) Steady value $\hat{\xi}'$ as a function of V_{v0} for the initial values $a_u=a_v=1.8$, $w_u=w_v=3.0$, $\xi_u=1.0$, $\xi_v=-1.0$, and $V_u=0.1$ with $\nu=500$, $q=2$, $A_u=1.0$, $A_v=0.95$, $D_u=1.0$, and $D_v=0.98$. Full numerical solution (+—+—+), solution of modulation equations (– – –), and solution of momentum conservation result (···).

aticons in the latter case experience a continual interaction with each other, but the profile shape change is much reduced. One reason for anharmonicity of the beam position oscillations is that beam distortions become amplified as accelerative and radiative effects take on a more significant role. These effects are more prevalent at lower values of ν, as can be seen in Fig. 3. The present approximate method cannot easily account for beam distortions since the beam profiles are fixed by the ansatz. Acceleration also cannot easily be incorporated into the approximate method since this would require the solution of a moving boundary value problem for which the boundary is unknown [25].

In the local limit the nematicons oscillate about each other for large z, with these oscillations gradually decreasing in amplitude, so that the two nematicons eventually have the same position [27]. In Fig. 2(a) the decay of the position oscillations is much less obvious, and it is not clear whether the beams eventually merge or continue oscillating as $z\to\infty$. Since the position oscillations do not appear to die away as z increases and the numerical solutions were anharmonic, the mean momentum deviation was found by taking a large final z and plotting the collision points of the colors. Linear regression was then applied to obtain the momentum deviation.

Figure 4 compares the mean momentum deviation $\hat{\xi}'$ for the two beams as a function of the initial velocity of the v color beam, V_{v0}, as given by the full numerical solution of the governing equations, the modulation solution, and the momentum conservation result (27). As for the local case [27], the agreement for momentum deviation between the numerical and modulation solutions is excellent. However, in the nonlocal limit momentum conservation result (27) is in much better agreement than in the local case [27]. The waveguide formed by the beams is much wider than the beams themselves in the nonlocal regime. The radiation then starts at the tail of the director beam rather than from the tail of the electric field beam [23]. Consequently this shed radiation has a lower amplitude, again as observed from experimental results [22]. Due to this effect, the nonlocal momentum deviation is well approximated by conservation result (27), in contrast to the local case [27].

IV. CONCLUSIONS

The interaction of two-color nematicons in the nonlocal response regime has been considered. Modulation equations governing the evolution of these nematicons were derived and excellent agreement with numerical solutions was found. Moreover better agreement was found for several aspects of the nematicon evolution than for the local response regime. It was additionally found that radiative losses and acceleration during collision decreased as the nonlocality of the nematic increased, in agreement with experimental observations. As a consequence, the agreement between the modulation and numerical solutions for the position oscillation was much better in both the amplitude and period than for the corresponding local limit case. In particular near perfect agreement between the modulation and numerical solutions for the momentum deviation of the combined vector nematicon was found. This near perfect agreement shows the utility of modulation theory as a modeling tool for studying optical devices based on the interaction of nematicons in a liquid crystal cell. This topic will be the subject of future research.

ACKNOWLEDGMENT

This research was supported by the Engineering and Physical Sciences Research Council (EPSRC) under Grant No. EP/C548612/1.

APPENDIX: SHELF RADIUS

The shelf radii, R_u and R_v, are determined by linearizing the modulation equations about their fixed point [21,23,24,26], assuming that $D_u=D_v$ and $A_u=A_v$, as dis-

cussed in Sec. II. Linearizing in this manner we obtain the simple harmonic oscillator equation for g_k,

$$g_k'' - \frac{\Theta \Lambda_k \hat{\Sigma}_k'}{I_1^2(\hat{w}_k^2 + 2\hat{a}_k \hat{w}_k \varphi)} g_k = 0, \tag{A1}$$

where

$$\hat{\Sigma}_k' = \hat{\sigma}_k' - \tfrac{1}{2} D_k \hat{V}_k^2,$$

$$\varphi = \frac{D_k I_{22} \Gamma^2 - A_k A^2 B^2 \hat{w}_k^2 \hat{\beta}_k^2 \Gamma (2\hat{\alpha}_k + \hat{a}_k W_1)}{A_k A^2 B^2 \hat{a}_k \hat{w}_k \hat{\beta}_k \Phi},$$

$$\Phi = 2A^2 \hat{\alpha}_k \hat{\beta}_k^3 + \hat{w}_k \hat{\beta}_k W_2 \Gamma + 2B^2 \hat{w}_k^3 \hat{\alpha}_k W_0,$$

$$\Gamma = A^2 \hat{\beta}_k^2 + B^2 \hat{w}_k^2, \quad W_1 = \frac{4A_k A^2 B^4 \hat{a}_k \hat{w}_k^4}{q(I_4 + A^2/4)\Gamma^2},$$

$$W_0 = \frac{2q(I_4 + A^2/4) B^2 \hat{w}_k \hat{\beta}_k^2 + \nu(8I_{42} + 1) B^2 \hat{w}_k}{2q\hat{\beta}_k (I_4 + A^2/4)(2A^2 \hat{\beta}_k^2 - B^2 \hat{w}_k^2)},$$

$$W_2 = \frac{8A_k A^4 B^4 \hat{a}_k^2 \hat{w}_k^3 \hat{\beta}_k}{q(I_4 + A^2/4)\Gamma^3} (\hat{\beta}_k - \hat{w}_k W_0),$$

$$\Theta = \frac{D_k I_{22}}{2\hat{w}_k^2} \left[P_0 - \frac{(P_1 + P_2)}{\hat{\alpha}_k \hat{w}_k \hat{\beta}_k} \right], \quad P_0 = 1 - \frac{2\hat{a}_k \varphi}{\hat{w}_k},$$

$$P_1 = \hat{w}_k \hat{\beta}_k [\hat{\alpha}_k + \hat{a}_k (W_1 + \varphi W_2)],$$

$$P_2 = 2\hat{\alpha}_k \hat{a}_k \varphi (A^2 \hat{\beta}_k^2 - B^2 \hat{w}_k^2)(\hat{\beta}_k - W_0)\Gamma^{-1}. \tag{A2}$$

As in Kath and Smyth [24], García-Reimbert *et al.* [20,26], and Minzoni *et al.* [23] the frequency of Eq. (A1) is matched to the nematicon oscillation frequency given by

$$\hat{\Sigma}_k' = 2A_k A^2 B^2 \hat{\alpha}_k \hat{w}_k^2 \hat{\beta}_k^2 (A^2 \hat{\beta}_k^2 - 2B^2 \hat{w}_k^2)(I_2 \Gamma^2)^{-1}, \tag{A3}$$

which results in

$$\Lambda_k = \frac{-\hat{\Sigma}_k' I_1^2 \hat{w}_k (\hat{w}_k + 2\hat{a}_k \varphi)}{\Theta}. \tag{A4}$$

[1] Y. S. Kivshar and G. P. Agrawal, *Optical Solitons: From Fibers to Photonic Crystals* (Academic, San Diego, 2003).
[2] A. Alberucci, M. Peccianti, G. Assanto, A. Dyadyusha, and M. Kaczmarek, Phys. Rev. Lett. **97**, 153903 (2006).
[3] C. Weilnau, M. Ahles, J. Petter, D. Träger, J. Schröder, and C. Denz, Ann. Phys. **11**, 573 (2002).
[4] M. Peccianti, C. Conti, G. Assanto, A. De Luca, and C. Umeton, Nature (London) **432**, 733 (2004).
[5] M. Peccianti, K. A. Brzdiakiewicz, and G. Assanto, Opt. Lett. **27**, 1460 (2002).
[6] C. Conti, M. Peccianti, and G. Assanto, Phys. Rev. Lett. **91**, 073901 (2003).
[7] G. Assanto, M. Peccianti, and C. Conti, Opt. Photonics News **14** (2), 45 (2003).
[8] G. Assanto and M. Peccianti, IEEE J. Quantum Electron. **39**, 13 (2003).
[9] G. Assanto, M. Peccianti, K. A. Brzdiakiewicz, A. de Luca, and C. Umeton, J. Nonlinear Opt. Phys. Mater. **12**, 123 (2003).
[10] C. Conti, M. Peccianti, and G. Assanto, Phys. Rev. Lett. **92**, 113902 (2004).
[11] N. Ghofraniha, C. Conti, and G. Ruocco, Phys. Rev. B **75**, 224203 (2007).
[12] M. Matuszewski, W. Krolikowski, and Y. S. Kivshar, Opt. Express **16**, 1371 (2008).
[13] C. Rotschild, B. Alfassi, O. Cohen, and M. Segev, Nat. Phys. **2**, 769 (2006).
[14] E. A. Kuznetsov and A. M. Rubenchik, Phys. Rep. **142**, 103 (1986).
[15] A. V. Mamaev, A. A. Zozulya, V. K. Mezentsev, D. Z. Anderson, and M. Saffman, Phys. Rev. A **56**, R1110 (1997).
[16] M. Segev, G. C. Valley, B. Crosignani, P. DiPorto, and A. Yariv, Phys. Rev. Lett. **73**, 3211 (1994).
[17] A. W. Snyder and D. J. Mitchell, Science **276**, 1538 (1997).
[18] Q. Guo, B. Luo, F. Yi, S. Chi, and Y. Xie, Phys. Rev. E **69**, 016602 (2004).
[19] A. Fratalocchi, M. Peccianti, C. Conti, and G. Assanto, Mol. Cryst. Liq. Cryst. **421**, 197 (2004).
[20] C. García-Reimbert, A. A. Minzoni, T. R. Marchant, N. F. Smyth, and A. L. Worthy, Physica D **237**, 1088 (2008).
[21] G. Assanto, N. F. Smyth, and A. L. Worthy, Phys. Rev. A **78**, 013832 (2008).
[22] A. Fratalocchi, A. Piccardi, M. Peccianti, and G. Assanto, Phys. Rev. A **75**, 063835 (2007).
[23] A. A. Minzoni, N. F. Smyth, and A. L. Worthy, J. Opt. Soc. Am. B **24**, 1549 (2007).
[24] W. L. Kath and N. F. Smyth, Phys. Rev. E **51**, 1484 (1995).
[25] N. F. Smyth and W. L. Kath, Phys. Rev. E **63**, 036614 (2001).
[26] C. García-Reinbert, A. A. Minzoni, and N. F. Smyth, J. Opt. Soc. Am. B **23**, 294 (2006).
[27] B. D. Skuse and N. F. Smyth, Phys. Rev. A **77**, 013817 (2008).
[28] T. R. Marchant and N. F. Smyth, J. Phys. A: Math. Theor. **41**, 365201 (2008).
[29] I. C. Khoo, *Liquid Crystals: Physical Properties and Nonlinear Optical Phenomena* (Wiley, New York, 1995).
[30] M. Peccianti, A. Dyadyusha, M. Kaczmarek, and G. Assanto, Phys. Rev. Lett. **101**, 153902 (2008).
[31] C. García-Reimbert, C. E. Garza-Hume, A. A. Minzoni, and N. F. Smyth, Physica D **167**, 136 (2002).
[32] C. García-Reimbert, A. A. Minzoni, N. F. Smyth, and A. L. Worthy, J. Opt. Soc. Am. B **23**, 2551 (2006).
[33] M. Peccianti, A. Fratalocchi, and G. Assanto, Opt. Express **12**, 6524 (2004).
[34] M. Peccianti, A. de Rossi, G. Assanto, A. De Luca, C. Umeton, and I. C. Khoo, Appl. Phys. Lett. **77**, 7 (2000).

[35] P. D. Rasmussen, O. Bang, and W. Królikowski, Phys. Rev. E **72**, 066611 (2005).
[36] W. Hu, S. Ouyang, P. Yang, Q. Guo, and S. Lan, Phys. Rev. A **77**, 033842 (2008).
[37] M. Abramowitz and I. A. Stegun, *Handbook of Mathematical Functions with Formulas, Graphs and Mathematical Tables* (Dover, New York, 1972).
[38] D. J. Kaup and A. C. Newell, Proc. R. Soc. London, Ser. A **361**, 413 (1978).
[39] B. Fornberg and G. B. Whitham, Philos. Trans. R. Soc. London, Ser. A **289**, 373 (1978).
[40] W. H. Press, S. A. Teukolsky, W. T. Vetterling, and B. P. Flannery, *Numerical Recipes in Fortran: The Art of Scientific Computing* (Cambridge University Press, Cambridge, 1992).
[41] W. Królikowski and O. Bang, Phys. Rev. E **63**, 016610 (2000).